Torque Ripple Reduction of the Torque Predictive Control Scheme for Permanent-Magnet Synchronous Motors

Hao Zhu, Xi Xiao, *Member, IEEE*, and Yongdong Li, *Member, IEEE*

***Abstract*—The direct torque control (DTC) technique of permanent-magnet synchronous motors (PMSMs) receives increasing attention due to its advantages in eliminating the current controllers and quicker dynamic response, compared with other motor control algorithms. However, high torque and stator flux ripples remain in the system when using DTC technologies. This means large stator voltage and current harmonic contents exist in the PM motors. Since the variation of motor electromagnetic torque is related to the voltages that are applied to the motor, by analyzing the relationships between stator flux, torque, and voltages, a PMSM torque predictive control scheme is proposed in this paper. In each digital signal processor cycle, the optimized voltage is utilized to reduce torque ripple, and the voltage vector angle is determined by the output of torque and flux hysteresis controllers. The proposed scheme is simulated and experimentally verified. Both simulation and experimental results have shown that low torque ripple and reduced stator current harmonics are achieved by using the proposed scheme.**

***Index Terms*—Permanent-magnet synchronous motor (PMSM), torque predictive control (TPC), torque ripple, voltage angle.**

NOMENCLATURE

R_s	Stator resistance.
L	Motor inductance.
i_s	Stator current.
u_s	Stator voltage.
ψ_s	Stator flux.
ψ_r	Rotor flux.
T_e	Electromagnetic torque.
ω	Rotor electrical speed.
ω_{N}	Rated electrical speed.
θ	Rotor position.
p	Operator d/dt.
p_n	Number of pole pairs.
J	Moment of inertia.
T_s	Digital signal processor (DSP) control cycle.
T_k	Time duration of voltage vector.

Manuscript received May 11, 2010; revised August 30, 2010 and February 23, 2011; accepted April 13, 2011. Date of publication May 27, 2011; date of current version October 18, 2011.

The authors are with the Department of Electrical Engineering, Tsinghua University, Beijing 100084, China (e-mail: h-zhu06@mails.tsinghua.edu.cn; xiao_xi@mail.tsinghua.edu.cn; liyd@mail.tsinghua.edu.cn).

Color versions of one or more of the figures in this paper are available online at http://ieeexplore.ieee.org.

Digital Object Identifier 10.1109/TIE.2011.2157278

I. INTRODUCTION

Permanent-magnet synchronous motors (PMSMs) have been receiving increasing attention in recent years. The invention of high-performance magnets, such as samarium cobalt and neodymium–boron–iron, makes it possible to achieve motor performances that can surpass the conventional direct current (dc) or induction motors. The advantages of PMSMs are high efficiency and reliance, high power factor and power density, good dynamic performance with high torque/inertia ratio, etc. Equipped with a proper control strategy, PMSMs are preferable in many of industrial, commercial, or domestic variable speed drive applications. In the mid-1980s, direct torque control (DTC) was introduced by Takahashi and Depenbrok as a new approach for torque and flux control of induction machines. Later, this concept is extended to other types of alternating-current machines drives [1]–[5]. In [1], a direct-torque-controlled PM machine drive was described; the flux and torque were regulated by the nonlinear hysteresis controllers. An optimum switching table was used to choose the voltage vector that maintains flux and torque within the limitation of the two hysteresis bands. In [6], the time delay due to data processing is discussed in detail, and a predictive solution is proposed. The right selection of the vector voltages allows a decoupled control of flux and torque without proportional–integral (PI) current regulators that field-oriented control (FOC) or vector control uses; thus, the torque response of the DTC is normally faster than that of the vector control. However, in every control cycle, the switching state of the inverter is updated only once, and the inverter state keeps unchanged, referring to the output of the hysteresis controllers. As a result, the torque ripple is relatively high, compared with those with vector control.

Torque ripple is a critical concern in many high-performance applications such as servo and traction drives, where low acoustic noise, high efficiency, or friendly human–machine interactions are highly demanded. The existence of torque ripple degrades the control accuracy of motor speed and makes the motor less stable. To overcome this problem, researchers have given great attention on reducing the torque ripple. In addition, many new DTC strategies are proposed. Multilevel inverter and matrix converter provides more voltage vectors in modulation; thus, lower torque ripple and lower harmonic content in the stator current can be expected [7], [8]. However, for the purpose of achieving lower ripples and almost fixed switching frequency, it is necessary to have an increasing amount of power switches. This will increase the complexity of the system and the

hardware cost. The selection of control voltage depends on the hysteresis bands of torque and flux controllers, which will introduce torque ripples to the motor. Other methods such as discrete space vector modulation have a similar problem [9], [10]. In a conventional DTC strategy, once the voltage vector is selected, its influence to the torque ripple cannot be controlled anymore. Predictive control provides a possibility to evaluate the performance of different voltage vectors, where a cost function is proposed to determine the right voltage vector that brings the lowest torque and flux ripple within one cycle [11], [12], or over a long period [13], [14]. However, in the proposed method, only basic voltages are taken into consideration, and the evaluation is a trial-and-test strategy, which gives no great contribution to diminishing the torque ripple.

The usage of limited number of voltage vectors is insufficient in accurate torque control. Then, a space-vector pulsewidth modulation (SVPWM)-based DTC scheme has been proposed, which shows to be an effective method to reduce the torque ripple [15], [16]. In the proposed method, an optimal reference voltage vector is calculated and applied to the machine using SVPWM. This application has been extended to multilevel inverter that has an increased number of voltage vectors, as demonstrated in [17]. The main drawback of the SVPWM-based DTC predictive control is that it employs an additional PI controller in calculating voltage control angle, and there will be transient torque overshooting if PI parameters are not properly adjusted [19]. In [20], a new torque predictive control strategy (hereafter referring to as TPC) is proposed. Unlike conventional DTC strategies that use look-up tables to select voltage vectors, the TPC strategy calculates the desired voltage vector based on torque mathematical equation for accurate torque control. This TPC strategy is proved to be superior to other DTC strategies [21], [22]. In this paper, a new TPC strategy is proposed. The relationships between motor torque, flux, and motor voltages are analyzed, and a new voltage vector predictive control equation is developed. The proposed scheme is verified by MATLAB simulation and is also experimentally verified with a three-phase surface-mounted PM motor.

This paper is organized as follows: In Section II, torque and stator flux expressions are presented with a surface-mounted PM synchronous motor in the stationary reference frame. The TPC strategy is discussed. Torque dynamic equation is derived for the PM motor with respect to the rotor flux, motor current, and voltage vectors, and a torque ripple reduction strategy is proposed. Sections III and IV give detailed simulation and experimental results to verify the proposed strategy. Conclusions are presented in Section V.

II. PMSM Model and TPC

A. PMSM Mathematical Model

The motor has to be appropriately modeled in order to analyze a PMSM variable speed driving system. For modeling the PM motor, assumptions are given as follows.

1) The neutral point is not connected.
2) Iron saturation is assumed negligible.
3) There are no eddy currents or core losses.
4) Only the fundamental wave of the air-gap field is considered for the calculation of the inductances.

In the analysis, the stationary reference frame is used. The electrical dynamics of the PMSM drive can be described in terms of vectors by the following equations.

Voltage equation:

$$\boldsymbol{u}_s = R\boldsymbol{i}_s + \frac{d}{dt}\boldsymbol{\psi}_s \tag{1}$$

Flux equation:

$$\boldsymbol{\psi}_s = L\boldsymbol{i}_s + \boldsymbol{\psi}_r \tag{2}$$

where $\boldsymbol{u}_s = [u_{s\alpha}\ u_{s\beta}]^t$, $\boldsymbol{i}_s = [i_{s\alpha}\ i_{s\beta}]^t$, $\boldsymbol{\psi}_s = [\psi_{s\alpha}\ \psi_{s\beta}]^t$, and $\boldsymbol{\psi}_r = [\psi_r \cos\theta\ \psi_r \sin\theta]^t$. Note that the d- and q-axes inductances are equal for a surface-mounted PM motor, and they are both represented by symbol L.

Motor electromagnetic torque is a function of the stator flux and the stator current. It can be expressed as

$$T_e = p_n \boldsymbol{\psi}_s \times \boldsymbol{i}_s. \tag{3}$$

B. Relationship of Voltage Vectors With the Motor Torque

For the analysis of TPC, it is necessary to obtain a discrete-time representation of the motor torque whose value is updated at every sampling interval. This is achieved based on motor mathematical equations.

From (3), the dynamic of the motor torque can be obtained as

$$\frac{d}{dt}T_e = p_n\left(\frac{d}{dt}\boldsymbol{\psi}_s \times \boldsymbol{i}_s + \boldsymbol{\psi}_s \times \frac{d}{dt}\boldsymbol{i}_s\right). \tag{4}$$

It is shown that the increment of the torque is a function of stator flux vector $\boldsymbol{\psi}_s$ and stator current vector $\boldsymbol{i}_s$. From (1) and (2), dynamic equations are obtained as follows:

$$\frac{d}{dt}\boldsymbol{\psi}_s = \boldsymbol{u}_s - R\boldsymbol{i}_s \tag{5}$$

$$\frac{d}{dt}\boldsymbol{i}_s = \frac{1}{L}\left(\boldsymbol{u}_s - R\boldsymbol{i}_s - \frac{d}{dt}\boldsymbol{\psi}_r\right). \tag{6}$$

Substituting (5) and (6) into (4), the torque dynamic can be derived as

$$\frac{d}{dt}T_e = \frac{p_n}{L}\boldsymbol{\psi}_s \times \boldsymbol{u}_s + p_n\boldsymbol{u}_s \times \boldsymbol{i}_s - \frac{R_s}{L}T_e - \frac{p_n}{L}\boldsymbol{\psi}_s \times \frac{d}{dt}\boldsymbol{\psi}_r. \tag{7}$$

By knowing the values of vectors $\boldsymbol{i}_s$, $\boldsymbol{\psi}_s$, and $\boldsymbol{\psi}_r$, it is possible to control the motor torque toward a desired value by controlling voltage vector $\boldsymbol{u}_s$. Suppose that during one DSP control cycle T_s, nonzero voltage vector $\boldsymbol{u}_s$ is applied to the motor with a time duration of T_k. Based on (7), the impact of this voltage vector to the motor torque can be derived as

$$\Delta T_e' = \left(\frac{p_n}{L}\boldsymbol{\psi}_s \times \boldsymbol{u}_s + p_n\boldsymbol{u}_s \times \boldsymbol{i}_s - \frac{R_s}{L}T_e - \frac{p_n}{L}\boldsymbol{\psi}_s \times \frac{d}{dt}\boldsymbol{\psi}_r\right)T_k. \tag{8}$$

For the rest time of the control cycle $T_s - T_k$, a zero voltage is applied; hence, the torque variation is deduced as

$$\Delta T_e'' = \left(-\frac{R_s}{L}T_e - \frac{p_n}{L}\boldsymbol{\psi}_s \times \frac{d}{dt}\boldsymbol{\psi}_r\right)(T_s - T_k). \tag{9}$$

The sum of (8) and (9) is the total torque increment in a full DSP control cycle T_s, as shown in the following:

$$\Delta T_e = \left(\frac{p_n}{L}\boldsymbol{\psi}_s \times \boldsymbol{u}_s + p_n \boldsymbol{u}_s \times \boldsymbol{i}_s\right) T_k + \left(-\frac{R_s}{L}T_e - \frac{p_n}{L}\boldsymbol{\psi}_s \times \frac{d}{dt}\boldsymbol{\psi}_r\right) T_s. \quad (10)$$

Equation (10) gives the relationship between voltage vector $\boldsymbol{u}_s$ and torque increment ΔT_e. In this equation, the values of stator and rotor fluxes are calculated based on the measurement of the stator current and the rotor speed. With calculated voltage vector $\boldsymbol{u}_s$ from this equation, TPC strategy can accurately control the motor torque.

C. Proposed TPC Strategy

If the output voltage vector $\boldsymbol{u}_s$ of the inverter satisfies (10), the torque error can be nullified in the next DSP control cycle. In order to simplify the control structure, in the TPC strategy, $\boldsymbol{u}_s$ is set with a fixed magnitude, which is equal to the magnitude of the basic voltage vector of the inverter. If the magnitude of voltage vector $\boldsymbol{u}_s$ is too small, it cannot assure a quick torque control response. On the other hand, the bigger the voltage is, the bigger the torque ripples will be. The time duration of voltage vector $\boldsymbol{u}_s$ uses a tested value of $0.7T_s$ according to the simulation and experiment results. Finally, by changing the direction of voltage vector $\boldsymbol{u}_s$, the increment of the torque and the stator flux can be properly controlled.

According to the mathematical model, the motor stator flux can be processed as an integration of voltages. Neglecting the voltage drop on stator resistance, the increment of the stator flux vector can be calculated as

$$\Delta \boldsymbol{\psi}_s = T_k(\boldsymbol{u}_s - R_s \boldsymbol{i}_s) \approx T_k \boldsymbol{u}_s. \quad (11)$$

With the above equation, the voltage vector in (10) can be approximately substituted by a stator flux error. The value of ΔT_e and $\Delta \psi_s$ are acquired from torque and flux hysteresis controllers. The calculation error of $\Delta \psi_s$ due to the approximation will introduce disturbance to the decision of the voltage vector control angle and, consequently, brings ripple to the control of motor electromagnetic torque. The TPC strategy in [22] also uses the stator flux vector $\boldsymbol{\psi}_s$ as a positioning reference, and the phase plane is divided into four parts to satisfy the control of the motor torque and the stator flux (see Fig. 1). The problem is that the calculation error of vector $\boldsymbol{\psi}_s$ will make the positioning become less accurate.

In order to overcome these problems, a new TPC strategy is proposed in this paper. As is known, the position angle of vector $\boldsymbol{\psi}_r$ is proportional to the value of rotor position angle, and this value can be acquired through a rotor position sensor. Taking vector $\boldsymbol{\psi}_r$ as a position reference, the control voltage can be more accurately oriented. To achieve this target, the relationship between $\boldsymbol{u}_s$ and $\boldsymbol{\psi}_r$ should be analyzed first. Rearranging the first part on the right side of (10), we have

$$\left(\frac{p_n}{L}\boldsymbol{\psi}_s \times \boldsymbol{u}_s + p_n \boldsymbol{u}_s \times \boldsymbol{i}_s\right) T_k = \left(\frac{p_n}{L}(\boldsymbol{\psi}_s - L\boldsymbol{i}_s) \times \boldsymbol{u}_s\right) T_k = \frac{p_n}{L}\boldsymbol{\psi}_r \times \boldsymbol{u}_s T_k. \quad (12)$$

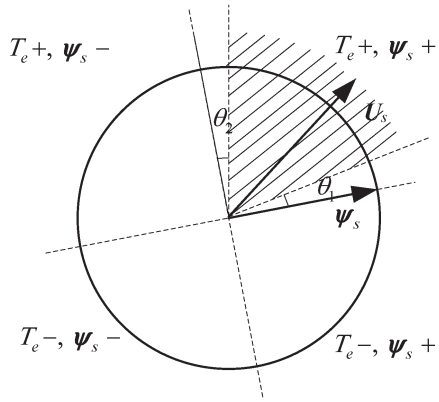

Fig. 1. Phase plane division for the control of torque and stator flux (TPC).

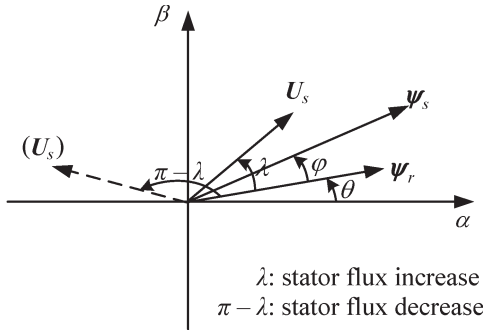

Fig. 2. Control of stator flux (proposed TPC).

Substituting (12) into (10) gets

$$\Delta T_e = \frac{p_n}{L}\boldsymbol{\psi}_r \times \boldsymbol{u}_s T_k + \left(-\frac{R_s}{L}T_e - \frac{p_n}{L}\boldsymbol{\psi}_s \times \frac{d}{dt}\boldsymbol{\psi}_r\right) T_s. \quad (13)$$

The calculation of ΔT_e in (13) is simplified, compared with (10). By knowing the magnitude of voltage vector $\boldsymbol{u}_s$, the new voltage control angle λ can be derived as follows:

$$\lambda = \arcsin\left(\frac{\Delta T_e + \left(\frac{R_s}{L}T_e + \frac{p_n}{L}\boldsymbol{\psi}_s \times \frac{d}{dt}\boldsymbol{\psi}_r\right) T_s}{\frac{p_n}{L}\,|\boldsymbol{\psi}_r|\,|T_k \boldsymbol{u}_s|}\right). \quad (14)$$

The purpose of angle λ is to decide the proper direction of voltage vector $\boldsymbol{u}_s$ for driving the torque error ΔT_e to zero. This angle λ is the phase difference between inverter voltage $\boldsymbol{u}_s$ and rotor flux $\boldsymbol{\psi}_r$ (see Fig. 2). Here, there is a need to point out that an angle with the value $\pi - \lambda$ also satisfies (13). This result is utilized in the control of the stator flux, as described in the next section.

A schematic of PMSM TPC system is shown in Fig. 3. There are two control loops that focus on the performance of the motor torque and flux, respectively. In the proposed control strategy, the motor torque and the stator flux are compared to their reference values. The differences are then sent to the predictive control block to calculate the control angle of voltage vector $\boldsymbol{u}_s$ according to (14). Finally, the control voltage $\boldsymbol{u}_s$ is generated from a two-level voltage source inverter to drive the PM motor, where the SVPWM method is used to control the switching of the inverter. The calculation of the control strategy is not complicated and can be carried out within one control cycle T_s, which is 0.1 ms in the simulation and the experiment.

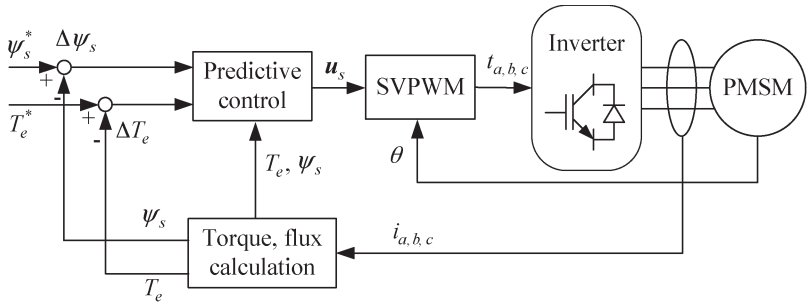

Fig. 3. Schematic of the PMSM speed regulation system based on torque predictive control.

D. Control of the Stator Flux

Angle λ of voltage vector $\boldsymbol{u}_s$ in (14) ensures an accurate control of the motor torque. Fig. 2 shows the vector relationship of $\boldsymbol{u}_s$, $\boldsymbol{\psi}_s$, and $\boldsymbol{\psi}_r$. As shown in this figure, $\boldsymbol{\psi}_s$ is leading phase angle φ before $\boldsymbol{\psi}_r$ so that a positive electromagnetic torque is generated. Angle φ becomes less than zero if negative torque is need. Additionally, the voltage vector $\boldsymbol{u}_s$ will change the magnitude of the stator flux. Once the phase difference between vectors $\boldsymbol{u}_s$ and $\boldsymbol{\psi}_s$ is within $\pm 90^\circ$, the magnitude of the stator flux will increase. Otherwise, the magnitude of the stator flux decreases. In most cases, the phase difference between $\boldsymbol{\psi}_s$ and $\boldsymbol{\psi}_r$ is small; therefore, when considering the control of the stator flux, the following voltage control angle λ' is used:

1) magnitude of the stator flux increases, let $\lambda' = \lambda$;
2) magnitude of the stator flux decreases, let $\lambda' = \pi - \lambda$.

Angle λ' is the final value of voltage vector $\boldsymbol{u}_s$ in the proposed new TPC strategy. Its value satisfies (13); thus, the motor torque is accurately controlled. The usage of this angle also ensures quick control of the stator flux magnitude.

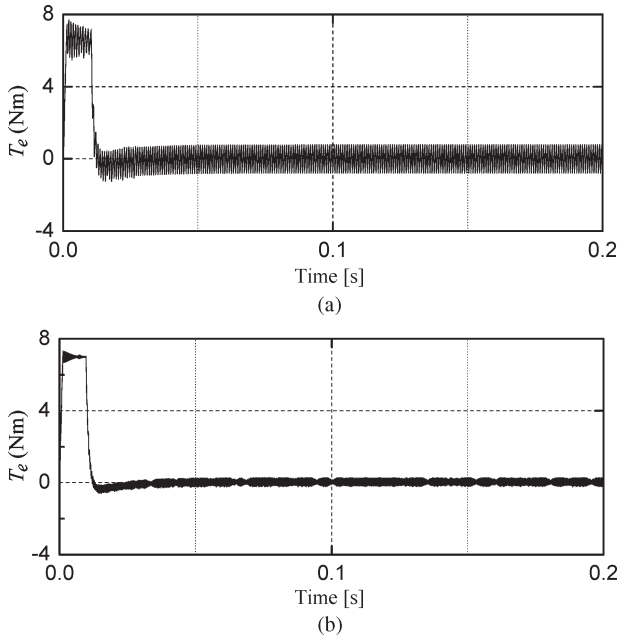

Fig. 4. Simulation result of the motor torque when the motor speed increases from 0 to 0.5 ω_{N}: (a) TPC and (b) proposed TPC.

III. Simulation Results

The performance of the proposed scheme is simulated by MATLAB/Simulink. A fixed-step simulation mode is used with a fundamental sample time of 0.1 ms in accordance with the experiment setting. Torque dynamic analysis and voltage control angle prediction are fulfilled in the simulation. A comparison of different TPC strategies is shown in Fig. 4. To test the dynamic response, a speed command from 0 to 0.4 ω_{N} is applied to the speed controller. As discussed in Section II, the advantage of the TPC strategy is that it can perform direct control of the motor torque. The vector control angle was precisely calculated for the voltage vector applied to the motor. This ensures quick tracing of torque reference once its value is changed. As shown in Fig. 4, both TPC strategies have a quick torque dynamic response. In addition, there is no torque overshoot like that in the FOC applications. In Fig. 4(a) and (b), the dynamic responses of two different schemes are intended to have close torque values over time. The major improvement of the proposed TPC strategy is that it provides a more accurate analysis about the torque increment. The calculation of voltage angle prediction is simplified, and fewer variables are involved. The simulation results in Fig. 4(b) show that the proposed TPC strategy effectively improves the torque control accuracy, where the torque ripple value is obviously smaller than that in Fig. 4(a). In a steady state, the average torque ripple has decreased from 0.8 to 0.2 Nm. This proves that the new TPC strategy has superior performance over the TPC strategy proposed in [21] and [22].

For verifying the superiority of the proposed TPC strategy over other torque direct control strategies, a comparison is made between the propose TPC and the SVPWM-based DTC [18]. Fig. 5 shows the torque dynamic response of the two strategies on step mutation of a given torque from -3 to $+3$ Nm. In the simulation, the speed command is 0.5 ω_{N}.

As shown in Fig. 5, both torque direct control strategies have a fast control response. This is the most important advantage against FOC. The difference is that there is less torque ripple when the proposed TPC strategy is used. Further researches have proven that the performance of the SVPWM-based DTC deeply depends on the coefficients of the additional PI controller used in the strategy. The torque dynamic error can be more than 0.5 times of its reference once the coefficients are not properly selected [18]. Nonetheless, the proposed TPC strategy does not cause such a problem; thus, more accurate dynamic torque response can be obtained.

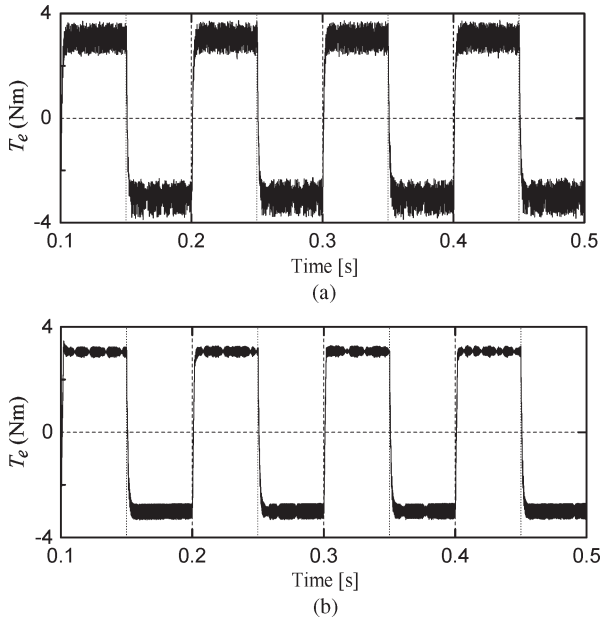

Fig. 5. Simulation result of the motor torque corresponding to a given torque step mutation from -3 to $+3$ Nm at 0.5 ω_N: (a) SVPWM-based DTC predictive control and (b) proposed TPC.

TABLE I
EXPERIMENTAL SETUP PARAMETERS

Parameter	Symbol	Value
Number of pole pairs	p	4
Rated power (kW)	P_N	1.5
Rated speed ($rad{\cdot}s^{-1}$)	ω_N	157.1
Rated frequency	f_N	100
Rated torque (Nm)	T_e	9.55
Rated voltage (V)	U_N	129
Rated current (A)	I_N	6.7
Stator inductance (mH)	L_s	9.52
Stator resistance (Ω)	R_s	0.123
Mechanical inertia ($kg{\cdot}cm^2$)	J	13.1
Back EMF constant ($N{\cdot}m/A$)	KE	1.43

IV. EXPERIMENTAL RESULTS

The effectiveness of the proposed TPC scheme is experimentally tested with an eight-pole 1.5-kW surface-mounted PM motor. Detailed motor parameters are tabulated in Table I. The sampling frequency for the predictive control scheme is 10 kHz. Control algorithm and data logging are programmed in a TMS320LF2812 DSP. The PM motor is fed by a two-level voltage source inverter. Hall-effect sensors (LEM 100-P/SP50 and CHV-25P) are used for current and voltage measurements, respectively. Three 10-bit on chip analog-to-digital conversion (ADC) channels are used for the ADC of the measured motor currents and dc bus voltage. A 2500 PPR incremental encoder is used to measure the rotor mechanical position. The coding of real-time control software is done using C language. The PWM signals are generated on the DSP board. A three-phase insulated-gate bipolar transistor intelligent power module is used for the VSI. An interface board and a host personal computer connected with the complex programmable logic device via serial interface are used as well.

Fig. 6 exhibits the load test results with different TPC strategies at the speed of 0.1 ω_N, where a 0.65-Nm load is applied to the motor. Remarkable torque ripples can be found with

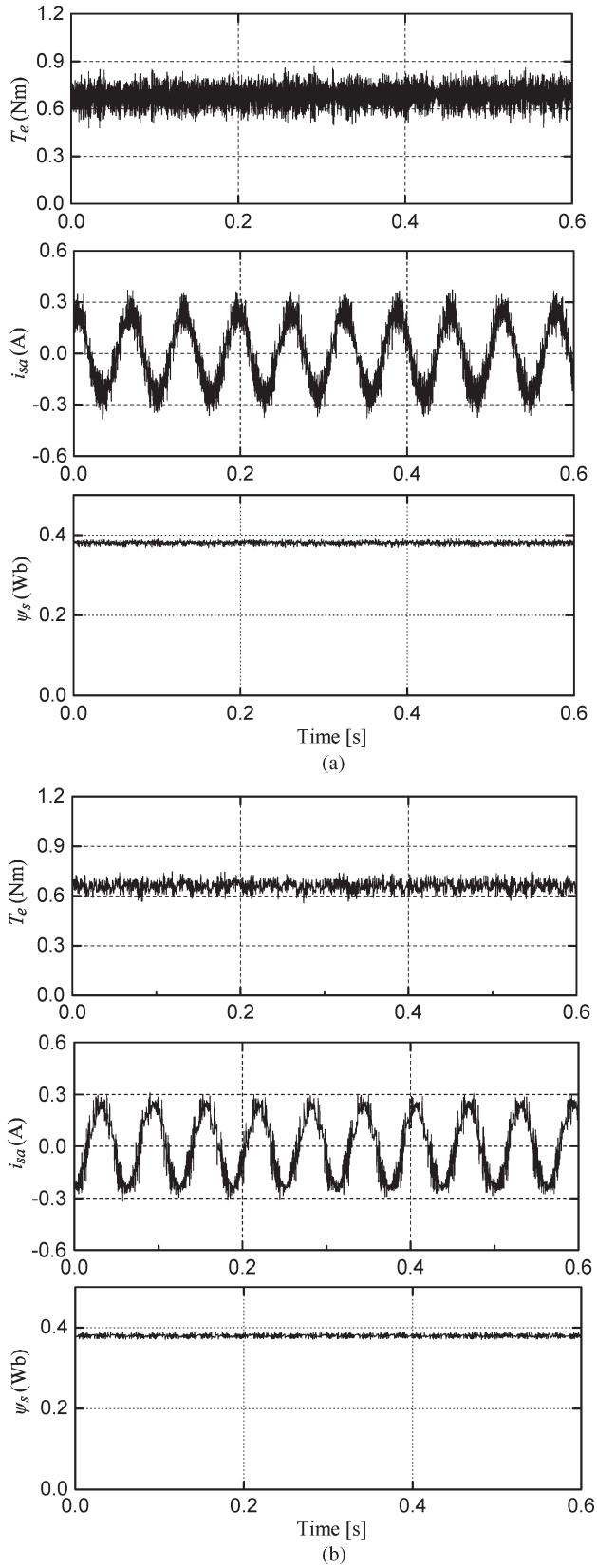

Fig. 6. Experimental results of torque, phase current, and stator flux at 0.5 ω_N: (a) TPC and (b) proposed TPC.

the TPC strategy, as shown in Fig. 6(a). In the experiment, the transient peak ripple is 0.18 Nm. This transient is quite comparable with the load torque. It is likely to influence motor

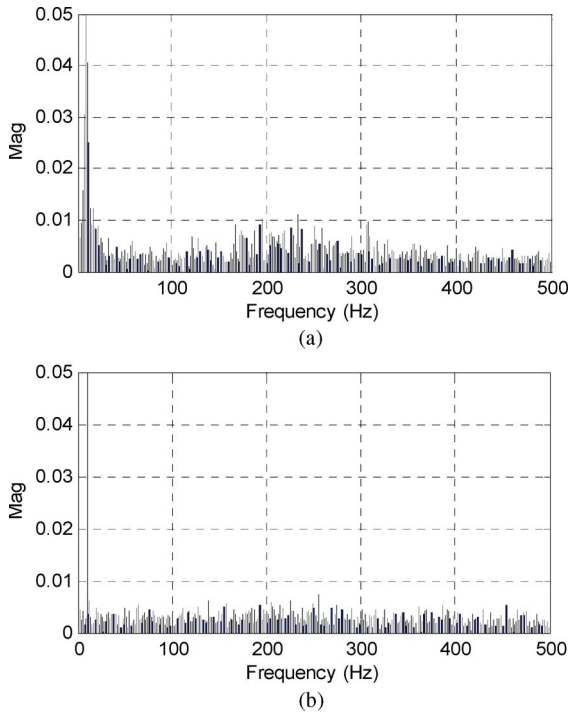

Fig. 7. Frequency spectra of the phase current at 0.5 ω_{N}: (a) TPC and (b) proposed TPC.

performance and bring acoustic noise while the motor is rotating. In Fig. 6(b), the proposed TPC strategy is used. The results show that the overall torque ripple is significantly reduced, with a maximum ripple of only 0.06 Nm. The same result is observed with the phase current. In the experiment, the proposed TPC strategy brings less current ripples, and the phase current shows good sinusoidal waveform.

The experimental results also proved good control performance with the stator flux of the TPC strategies. In the experiment, the magnitude reference of the stator flux is 0.3812 Wb. It is shown that the magnitude of the flux in Fig. 6 is very close to their reference value, and only slight flux magnitude ripple can be found. Both strategies ensure high accuracy control about the stator flux. Referring to (11), it can draw a conclusion that the magnitude increment of the stator flux is less than the product of u_s and T_s. For example, in the experiment, u_s is set as 100 V, and the DSP control cycle is 0.1 ms; then, $\Delta\psi_s$ will be less than 0.01 Wb in each control step. There will be no sharp magnitude changing of the stator flux.

The frequency spectra for phase current using different TPC strategies are shown in Fig. 7. In Fig. 7(a), the magnitude of the fundamental component is 0.2401 A. This is almost the same as that in Fig. 7(b), whose magnitude is 0.2396 A. In Fig. 7(a), the spectrum of the phase current when using the TPC strategy contains prominent harmonics that widely distribute around the fundamental frequency, and the maximum harmonic is nearly 0.04 A. As shown in Fig. 7(b), the overall harmonic components stay at a relatively low level when using the proposed TPC strategy, particularly, the harmonic components near the fundamental term have been greatly reduced. The maximum value of harmonic components is 0.007 A. This is much smaller than that shown in Fig. 7(a).

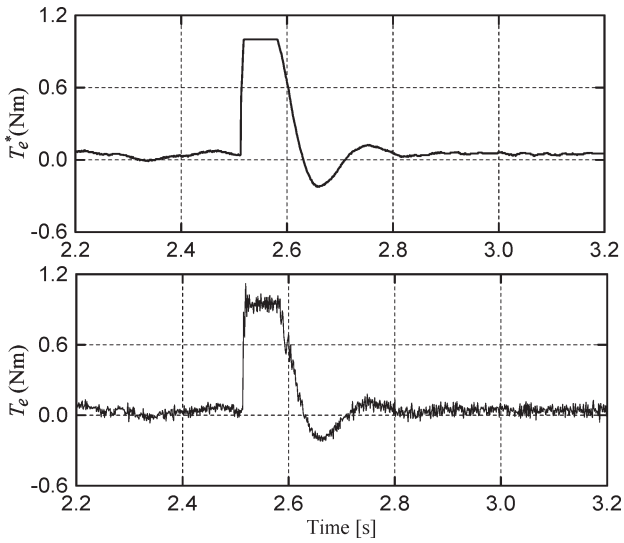

Fig. 8. Experimental result of the motor torque when the motor speed increases from 0.1 to 0.6 ω_{N} (proposed TPC).

The most important advantage of using the TPC strategy is the fast dynamic torque response. Fig. 8 is the experimental result of torque dynamic control performance using the proposed TPC strategy with a speed step changed from 0.1 to 0.6 ω_{N}. As speed reference changes, the output of the speed PI accordingly varies, and a time-varying torque command is given to the close-loop control system. In the experiment, the torque reference is limited with a maximum value of 1 Nm. As can be expected, torque reference changes from zero to upper limit within a very short time period. Once the measured speed matches the desired reference value, the torque drops to zero, and the machine runs at constant speed. It is shown that the motor torque is fully controlled to track its reference curve both at dynamic and steady states. The torque error is small and negligible when the motor is operating at a steady state.

V. Conclusion

In this paper, a TPC strategy has been discussed based on the discrete-time state-space model of the PMSM. A torque dynamic equation is developed for the analysis of torque real-time behavior. The prediction scheme uses incremental changes in the stator flux and the stator current, together with voltage vectors to achieve accurate torque control. Then, a new voltage-vector-based TPC strategy is proposed. Instead of using the increment of stator flux magnitude that might introduce deviation to the calculation, voltage vector is directly handled in the prediction of voltage control angle. Moreover, the control voltage is accurately oriented according to rotor flux vector. This extended prediction scheme not only simplifies the calculation but also effectively improves the calculation accuracy. Combined with flux control criteria that follows the principle of DTC, the voltage vector control angle is carefully selected to deliver high control performance of both the torque and the stator flux. The simulation and experimental results have demonstrated the feasibility of the new TPC system with fast dynamic torque response, low torque ripple, and sinusoidal behavior of the stator current.

REFERENCES

[1] M. F. Rahman, D. E. Haque, L. Tang, and L. Zhong, "Problems associated with the direct torque control of an interior permanent-magnet synchronous motor drive and their remedies," *IEEE Trans. Ind. Electron.*, vol. 51, no. 4, pp. 799–809, Aug. 2004.

[2] F. Bonnet, P. E. Vidal, and M. Pietrzak-David, "Dual direct torque control of doubly fed induction machine," *IEEE Trans. Ind. Electron.*, vol. 54, no. 5, pp. 2482–2490, Oct. 2007.

[3] L. Zheng, J. E. Fletcher, B. W. Williams, and X. He, "A novel direct torque control scheme for a sensorless five-phase induction motor drive," *IEEE Trans. Ind. Electron.*, vol. 58, no. 2, pp. 503–513, Feb. 2011.

[4] G. H. B. Foo and M. F. Rahman, "Direct torque control of an IPM-synchronous motor drive at very low speed using a sliding-mode stator flux observer," *IEEE Trans. Power Electron.*, vol. 25, no. 4, pp. 933–942, Apr. 2010.

[5] S. B. Ozturk, W. C. Alexander, and H. A. Toliyat, "Direct torque control of four-switch brushless dc motor with non-sinusoidal back EMF," *IEEE Trans. Power Electron.*, vol. 25, no. 2, pp. 263–271, Feb. 2010.

[6] J. Beerten, J. Verveckken, and J. Driesen, "Predictive direct torque control for flux and torque ripple reduction," *IEEE Trans. Ind. Electron.*, vol. 57, no. 1, pp. 404–412, Jan. 2010.

[7] K. E. B. Quindere, E. F. Ruppert, and M. E. F. de Oliveira, "Direct torque control of permanent magnet synchronous motor drive with a three-level inverter," in *Proc. Power Electron. Spec. Conf.*, Jun. 2006, pp. 1–6.

[8] C. Ortega, A. Arias, C. Caruana, J. Balcells, and G. M. Asher, "Improved waveform quality in the direct torque control of matrix-converter-fed PMSM drives," *IEEE Trans. Ind. Electron.*, vol. 57, no. 6, pp. 2101–2110, Jun. 2010.

[9] D. Ocen, L. Romeral, J. A. Ortega, J. Cusido, and A. Garcia, "Discrete space vector modulation applied on a PMSM motor," in *Proc. Power Electron. Spec. Conf.*, Jun. 2006, pp. 320–325.

[10] B. Singh and D. Goyal, "Improved DSVM-DTC based current sensorless permanent magnet synchronous motor drive," in *Proc. PEDS*, Nov. 2007, pp. 1354–1360.

[11] H. Miranda, P. Cortes, J. I. Yuz, and J. Rodriguez, "Predictive torque control of induction machines based on state-space models," *IEEE Trans. Ind. Electron.*, vol. 56, no. 6, pp. 1916–1924, Jun. 2009.

[12] F. Morel, L.-S. Xuefang, J. M. Retif, B. Allard, and C. Buttay, "A comparative study of predictive current control schemes for a permanent-magnet synchronous machine drive," *IEEE Trans. Ind. Electron.*, vol. 56, no. 7, pp. 2715–2728, Jul. 2009.

[13] T. Geyer, G. Papafotiou, and M. Morari, "Model predictive direct torque control—Part I: Concept, algorithm, and analysis," *IEEE Trans. Ind. Electron.*, vol. 56, no. 6, pp. 1894–1905, Jun. 2009.

[14] G. Papafotiou, J. Kley, K. G. Papadopoulos, P. Bohren, and M. Morari, "Model predictive direct torque control—Part II: Implementation and experimental evaluation," *IEEE Trans. Ind. Electron.*, vol. 56, no. 6, pp. 1906–1915, Jun. 2009.

[15] Y. Inoue, S. Morimoto, and M. Sanada, "Examination and linearization of torque control system for direct torque controlled IPMSM," *IEEE Trans. Ind. Appl.*, vol. 46, no. 1, pp. 159–166, Jan./Feb. 2010.

[16] G. Foo and M. F. Rahman, "Sensorless direct torque and flux-controlled IPM synchronous motor drive at very low speed without signal injection," *IEEE Trans. Ind. Electron.*, vol. 57, no. 1, pp. 395–403, Jan. 2010.

[17] S. Kouro, R. Bernal, H. Miranda, C. A. Silva, and J. Rodriguez, "High-performance torque and flux control for multilevel inverter fed induction motors," *IEEE Trans. Ind. Electron.*, vol. 22, no. 6, pp. 2116–2123, Nov. 2007.

[18] L. Tang, L. Zhong, and M. F. Rahman, "A novel direct torque control for interior permanent-magnet synchronous machine drive with low ripple in torque and flux-a speed-sensorless approach," *IEEE Trans. Ind. Appl.*, vol. 39, no. 6, pp. 1748–1756, Nov./Dec. 2003.

[19] M. Pacas and J. Weber, "Predictive direct torque control for the PM synchronous machine," *IEEE Trans. Ind. Electron.*, vol. 52, no. 5, pp. 1350–1356, Oct. 2005.

[20] H. Hu and Y. Li, "A predictive direct torque control strategies of induction motor based on area voltage vector table," *Trans. China Electrotech. Soc.*, vol. 19, no. 2, pp. 25–30, Feb. 2004.

[21] Y. Li, C. Wang, and H. Hu, "Predictive control of torque and flux of induction motor drives," in *Proc. PEDS*, Nov. 2005, pp. 67–71.

[22] M. Zhang, X. Xiao, and Y. Li, "Predictive direct torque control of PM synchronous motors based on an area voltage vector table," *J. Tsinghua Univ.*, vol. 48, no. 1, pp. 25–30, Jan. 2008.

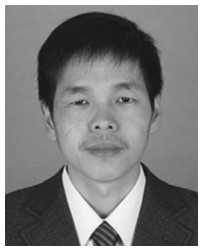

Hao Zhu was born in Jiangsu, China, in 1979. He received the B.S. degree from North China Electrical Power University, Beijing, China, in 2002 and the M.S. degree in 2005 from Tsinghua University, Beijing, where he is currently working toward the Ph.D. degree in the Department of Electrical Engineering.

His current research interests are power-electronic control of electric machines and power-converter circuits.

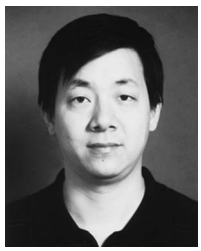

Xi Xiao (M'XX) was born in Hunan Province, China, in 1973. He received the B.E., M.E., and Ph.D. degrees from Saint Petersburg State Technical University, Saint Petersburg, Russia, in 1995, 1997, and 2000, respectively.

Since 2001, he has been with the Department of Electrical Engineering and Applied Electronic Technology, Tsinghua University, Beijing, China, where he is currently an Associate Professor. His main areas of research interest are permanent-magnet synchronous motors for servo drive applications and power electronics.

Yongdong Li (M'08) was born in Hebei, China, in 1962. He received the B.S. degree from Harbin Institute of Technology, Harbin, China, in 1982, and the M.S. and Ph.D. degrees from the Institut National Polytechnique de Toulouse, Toulouse, France, in 1984 and 1987, respectively.

He has been a Professor since 1996 and a Ph.D. Student Supervisor since 1999 with the Department of Electrical Engineering, Tsinghua University, Beijing, China. In 1995, he was a Visiting Scholar with the Department of Electrical Engineering, Yokohama National University, Yokohama, Japan. From June to December 1996, he was a Visiting Professor with Virginia Power Electronics Center, Virginia Polytechnique Institute and State University, Blacksburg. In 2002, he was an Invited Professor of the Institut National Polytechnique de Toulouse. He has authored or coauthored more than 200 papers and two monographs on digital control of alternating current (ac) motor and on multilevel converter. His main research interests include control theories, real-time implementation, sensorless drives and applications of vector and direct torque control of ac motors, and high-voltage and high-power inverters for motor drives and active power filter application.

Dr. Li is a Senior Member of the China Electro-Technique Society, the Vice-Chairman of the China Power Electronics Society, and the Vice-Chairman of the Electrical Automation Committee of China Automation Association.